CARBON SOOT AS A POTENTIAL AND SUSTAINABLE SOURCE OF POROUS NANOSTRUCTURE FOR ENERGY STORAGE

A thesis presented to the Department of Material Science and Engineering
African University of Science and Technology, Abuja
In partial fulfilment of the requirements for the award

MASTER OF SCIENCE

By

ATTAH CHIMA PASCHAL
Supervised by
Dr. Bello Abdulhakeem

African University of Science and Technology
www.aust.edu.ng
P.M.B 681, Garki, Abuja F.C.T
Nigeria

November 2017

CARBON SOOT A POTENTIAL AND SUSTAINABLE SOURCE OF POROUS NANOSTRUCTURE FOR ENERGY STORAGE

By

Attah Chima Paschal

A THESIS APPROVED BY THE MATERIAL SCIENCE AND ENGINEERING DEPARTMENT

RECOMMENDED: ----------

Supervisor, Bello Abdulhakeem

Co-Supervisor, Prof. M.G. Zebaze Kana

Head of Department, Prof. Onwualu Peter

APPROVED: ----------

Chief Academic Officer

Date

CERTIFICATION

This is to certify that the thesis titled “Carbon Soot a Potential and Sustainable Source of Porous Nanostructure for Energy Storage” submitted to the school of postgraduate studies, African University of Science and Technology (AUST), Abuja Nigeria for the award of the Master's degree is a record of original research carried out by Attah Chima Paschal in the Department of Material Science and Engineering.

ABSTRACT

There is a need for efficient energy storage to meet the world's continuous demand for energy. The electrical energy storage devices available are conventional capacitors, electrochemical supercapacitors, batteries and fuel cells. The electrode materials play an important role in improving the efficiency of energy storage systems such as batteries and electrochemical supercapacitors. The electrochemical supercapacitors have power densities greater than those of batteries, energy densities greater than those of conventional capacitors and also maintain high cyclic life. Despite these advantages, electrochemical supercapacitors do not offer sufficient energy densities compared to batteries and fuel cells. Therefore, there is a need for research to improve the performance of electrochemical supercapacitors without compromising on their power densities and cycle life. This work explores the use of carbon soot as a potential and sustainable source of porous activated carbon materials and as an electrode for supercapacitors. This is because soot is produced in the combustion chambers of vehicles and is readily available and abundant. Thus, we explored carbon soot as a potential electrode material for supercapacitors using potassium bicarbonate as the activating agent and the activated carbon displayed a specific surface area of 61.85 m^2 g^{-1} and a capacitance of 83.2 F g^{-1} at the low current density of 0.5 Ag^{-1}. This result demonstrates the potential of this source of activated carbon for electrochemical applications.

Keywords: Supercapacitor Energy Storage, Pseudocapacitance, Electrochemical double-layer, carbon soot

ACKNOWLEDGMENT

I sincerely acknowledge the tireless effort of my supervisor Dr. Bello for his encouragement, tenderness and sublime patience that enabled me to complete this thesis. I would not have done much without his supervision. I am indebted to him for he did much for me beyond thesis supervision, he always had my future interests at heart. I also appreciate the effort of Prof. M.G. Zebaze Kana for his input in the completion of this work.

I am grateful to the head of department Prof. Azikiwe Peter Onwualu for his fatherly support throughout our Master's program. I also appreciate the impact of all Pan African Material Institute (PAMI) center leaders to our great institution. I appreciate the African Development Bank (ADB) for the scholarship they awarded to me.

I am thankful for my best friend, Eng. Ezema Abraham without whom I would be ignorant of the existence of this great institution, he has also impacted my life in a way that he can never understand. I also appreciate Sis Maria for her encouragement and inspiration, it helped me to stand firm during my difficult time in school.

My sincere gratitude goes to my friends in my department Chukwudalu Nwazojie, Abraham Ebunu, David, Ridwan, Yusuf, Daniel, Chinenye, Sandra, Josiah, Killian, Ifeyinwa, Lilian, Maryam, Kabirat, and my humble class representative Olugbenga Ayeni for teaching me how to be a team player.

Finally, I thank my parents for their sacrifice and also to my niece and only sister Egbo Chidimma and my new-born nephew Chiemeria, may the almighty God bless you all. Amen.

DEDICATION

To God almighty and to my parents who made a huge sacrifice for my life, I dedicate this work.

TABLE OF CONTENTS

LIST OF FIGURES

LIST OF TABLES

LIST OF ACRONYMS

AC Activated carbon

BF4 Tetrafluoroborate

BET Brunauer–Emmett–Teller

CAE Compressed air electric storage

S CE Counter electrode

C2H2 Acetylene

CNTs Carbon nanotubes

CP Conducting polymer

DCA Dicyanamide

EDLC Electric double-layer capacitors

EES Electrical energy storage

EV Electric Vehicle

FES Flywheel electric storage

FTIR Fourier-transform infrared spectroscopy

GPE Gel polymer electrolytes

HACA Hydrogen abstraction and carbon addition

HEV Hybrid Electric Vehicle

ICE Internal combustion engines

IR Infrared radiation

IUPAC International Union of Pure and Applied Chemistry

MWCNTs Multiple wall carbon nanotube

NMP N-Methylpyrrolidone

PAA Poly (acrylic acid)

PAAK Potassium polyacrylate

PAH Polyaromatic hydrocarbons

PANI Polyaniline

PF6 Hexafluorophosphate

PF6 Hexafluorophosphate

PHS Pumped hydroelectric storage (PHS),

PEEK Polythiophene

PEDOT Poly (3,4-ethylene dioxythiophene)

Hexafluorophosphate (PF6)

PEO Poly (ethyl oxide)

PMMA Poly-(methylmethacrylate)

PPy Polypyrrole

PTH Polythiophene

PPV Poly (p-phenylene vinylene)

PVA Vinyl alcohol

PVDF Polyvinylidene difluoride

SCs Supercapacitors

SEM Scanning Electron Microscopy (SEM)

SMES Superconducting magnetic energy storage

SoC State of charge

SPE Solid polymer electrolytes

SWCNTs Single wall carbon nanotube

MWCNTs Multiple wall carbon nanotube

RE Reference electrode

TMOs Transition Metal Oxides

TFSI bis(trifluoromethane sulfonyl)imide

WE Working electrode

CHAPTER ONE

1.0 Introduction

1.1 Background

Energy is a global challenge due to the increase in environmental pollution and ozone layer depletion as a result of the burning of fossil fuels which are the chief source of conventional energy. As a consequence, there is a high demand for clean and renewable energy sources as direct alternatives to fossil fuels in order to foster sustainable and pollution free environments. (Liu, Li, Ma, & Cheng, 2010). Energy storage is an efficient use of energy because it is clean and sustainable. There are various types of energy storage systems such as batteries, conventional capacitors, supercapacitors, fuel cells pumped hydroelectric storage (PHS), compressed air electric storage (CAES), and flywheel electric storage (FES). There has been ongoing research in the development of advanced energy storages devices such as supercapacitors (Ellenbogen, 2006).

Supercapacitors (SCs), also known as ultracapacitors or electrochemical capacitors are electrical energy storage devices that utilize higher surface area electrode materials to achieve greater capacitances. The SCs have energy densities greater than those of conventional capacitors and power densities greater than those of batteries. Therefore, they bridge the gap between the conventional capacitor and batteries. The energy storage of a supercapacitor per unit volume or mass is 10 to 100 times more than the conventional capacitor and it also withstands more charging and discharging cycles than batteries (Conway, 1999). Electrochemical SCs are classified into electric double-layer capacitors (EDLC), pseudocapacitors and hybrid supercapacitors (Abruña, Henderson, & Kiya, 2008) (Béguin, Raymundo-Piñero, & Frackowiak, 2009). The applications of SCs in the advanced energy storage technology are currently under intense research.

They can be used in place of batteries in technology where high power and energy density is needed, for example portable electronics and electric vehicles. Significant improvement in the performance of supercapacitors has been achieved by advanced nanostructured electrode materials such as activated carbon, conducting polymers and transition metal oxides. (Li, Yang, & Zhitomirsky, 2010).

Porous carbon materials such as activated carbon are efficient for hydrogen storage adsorbents and electrode materials in SCs application due to their variable microstructure, large specific surface area (SSA), variation in forms, and availability. They are also sustainable and environmentally friendly (J. Wang & Kaskel, 2012). Physical and chemical activation is the common procedure for the production of carbon material. Physical activation involves the removal of non-carbon elements by carbonization of carbon precursors in an inert atmosphere. Porosity is developed at the temperature of 600-1200 ^{o}C by activation in the presence of proper oxidizing gasifying agents such as O_2, CO_2 or steam. In chemical activation, reagents like potassium hydroxide (KOH) are used as an activation reagent because of its definite microspore size distribution, the ultra-high specific surface area which is up to 3000 m^2 g^{-1} and pore volume (PV) of over 2 cm^3 g^{-1} (J. Wang & Kaskel, 2012).

1.2 Statement of the Problem

SCs are storage devices that have high charging and discharging rates as a result of a high power density and can withstand a million charge and discharge cycles without loss of energy storage capacity. In spite of these excellent properties, the major problem of SCs is the low energy density which means that the quantity of energy they store per unit weight is very small when compared to their battery counterpart. Therefore, there is need to research into new materials and methods to improve the energy density of SCs.

This can be achieved by looking at new and sustainable routes to porous carbon materials and optimizations in various aqueous electrolytes as efficient electrodes.

1.3 Objectives

- ➢ To explore carbonaceous soot as a suitable and sustainable source of activated carbon.
- ➢ To explore the AC as a potential electrode material for SCs.
- ➢ To optimize the electrochemical performance of the produced AC in aqueous electrolyte.

1.4 Scope

- ➢ Chapter two covers the overview of SCs, and their current development as advanced energy storage systems.
- ➢ Chapter three involves research methods and experimental characterization with state-of-the-art facilities such as SEM, FTIR, gas absorption analysis and electrochemical experiment.
- ➢ Chapter four is the analysis of experimental results.
- ➢ Chapter five presents the conclusion and recommendations.

CHAPTER TWO

2.0 Literature Review

2.1 Energy Storage Development

Effective methods of energy storage have been under intense research since the discovery of electricity. Electrical energy storage (EES) is the process of converting electrical energy from a power source to a form that can be stored in various mediums (Chen et al., 2009). The stored energy can be converted to electrical energy when there is a need for electricity. The EES serves many functions in the power sectors such as:

I. Enhancing power reliability
II. Helping in management of power distribution
III. Reducing the intermittence of renewable power sources
IV. Improving time-varying energy management (Luo, Wang, Dooner, & Clarke, 2015)

2.2 Classification of Electrical Energy Storage Technologies

Electrical energy storage technologies can be classified into six categories based on the form of energy stored in the system and they are:

(1) Mechanical: pumped hydroelectric storage (PHS), compressed air electric storage (CAES) and flywheel electric storage (FES)
(2) Electrochemical: Batteries
(3) Electrical: Capacitors and supercapacitors, superconducting magnetic SMES
(4) Thermochemical: solar fuels
(5) Chemical: fuel cells (Luo et al., 2015)

2.2.1 Mechanical Storage system

The mechanical storage system of electricity is classified into pumped hydroelectric energy storage (PHES), compressed air energy storage (CAES) and flywheel energy storage (FES) (Chen et al., 2009).

2.2.1.1 Pumped Hydroelectric Energy Storage (PHES)

The PHES is majorly used by electrical power systems for load balancing. It uses the gravitational potential energy of water, to generate electricity. During the off-peak hour, water is pumped from the lower reservoir to the upper reservoir (charging process) for storage. When electricity is needed, water flows back from the upper to lower reservoir and powers the turbine to generate electricity (discharging process). The PHES has advantages of a high efficiency of 70% to 80% and unlimited cycle stability. The major disadvantages of PHES are initial capital cost and its site-specific (Luo et al., 2015).

2.2.1.2 Compressed Air Energy Storage (CAES)

This uses the potential energy of a compressed gas to generate electrical energy. Electricity is initially used to compress air and stores it in an underground system vessel or storage carven (Gardner, 2007). When electricity is needed, the stored compressed gas is expanded through the conventional gas turbine expander to generate energy. For maximum energy generation, the compressed air is mixed with natural gas. This technology enhances the green energy generations. The downside of this system is that the energy being supplied to the grid is less than the one supplied without the storage system (Luo et al., 2015).

2.2.1.3 Flywheel Energy Storage (FES)

Rotational energy is stored in this system by the acceleration of rotor or flywheel at a very high speed. When this stored energy is extracted, the speed of the flywheel decreases as a result of conservation of energy (Luo et al., 2015).

The rotor of a FES system is made of a carbon-fiber composite which is suspended by a magnetic bearing. It rotates at a speed range between 20,000 to over 50,000 rpm inside a vacuum (Castelvecchi, 2009). A transmission device is used to supply electricity to accelerate the flywheel but if the rotation of the flywheel is reduced, electricity is extracted through the same transmission device (Sung et al., 2002).

2.2.2 Electrochemical (Batteries)

Batteries are an electrochemical storage device which consist of one or more cells connected in series or parallel that store chemical energy and later convert it into electrical energy when needed. Batteries usually consist of at least one voltaic cell that is composed of oxidation and a reduction half-cell separated by a semipermeable membrane (salt bath). Each half-cell contains a metal electrode (cathode and anode); oxidation occurs at the anode while reduction occurs at the cathode. This means that the anode losses electrons while the cathode gains electrons. The two electrodes are submerged in an electrolyte which is composed of ions. The movement of electrons from the anode to the cathode generates energy that powers the battery.

They are classified into primary and secondary batteries. The primary batteries are deposable and non-chargeable as a result of non-reversible electrochemical reactions. The secondary batteries are rechargeable due to their reversible electrochemical reactions. Batteries can be classified as wet and dry cells. The wet cells are composed of a liquid electrolyte and it uses insulator sheets to separate the anode and cathode.

Examples of wet cell batteries are Leclanche cells, Daniel cells lead-acid accumulator etc. The dry cell contains paste as the electrolytes.

2.2.3 Thermochemical Energy Storage

–Thermochemical energy storage is the storage of heat energy in a chemical bond. It uses a reversible chemical reaction to absorb heat that is stored in the form of energy (Abedin & Rosen,

2011). Examples of thermochemical energy storage devices are solar fuels and solar hydrogen. (Luo et al., 2015). Solar fuel is a technology that uses thermal energy from the sun to convert carbon dioxide, water, and nitrogen into synthetic fuel. It stores solar energy in the form of chemical bonds (Lin, Rothensteiner, Alxneit, van Bokhoven, & Wokaun, 2016). The synthetic chemical fuel can be produced either directly or indirectly from solar energy (sunlight or solar heat) through photochemical, thermochemical and electrochemical reaction. It offers sustainable energy with no net emission of carbon dioxide (Hammarström & Hammes-Schiffer, 2009).

2.2.4 Chemical Storage (Fuel Cell)

The fuel cell is a storage device that stores chemical energy from fuel and converts it to electricity through an electrochemical reaction of the hydrogen-containing fuel with oxygen or other oxidizing agents. The fuel cell needs a continuous supply of fuel and oxygen mostly from air to maintain chemical reaction (Kumar, Agarwal, & Gupta, 2011). The fuel cell is composed of an electrolyte sandwiched between the electrode (anode) and an oxidant electrode (cathode) as the three actives component. The electrode of the fuel cell is made of porous material (Sharaf & Orhan, 2014).

2.2.5 Electrical

This includes the conventional capacitors and double-layer capacitors or supercapacitors.

2.2.5.1 Capacitors

A capacitor is a passive two-terminal energy storage device. It stores energy in the form of an electrical charge and produces a static voltage or a potential difference across its plates. A capacitor is composed of two parallel conducting plates that are electrically separated by insulating material like ceramic, mica, waxed paper, liquid gel and air (Alexander & Sadiku, 2007).

2.2.5.2 Supercapacitors

Supercapacitors also known as ultracapacitors differ from conventional capacitors because they offer greater capacitance than the conventional capacitors and store energy from electrochemical reactions, unlike the conventional capacitors that store energy by means of static charge.

The major attributes of SCs as energy storage devices is their high power density which is up to 10 kW kg^{-1} and limited energy density value which is < 10 W kg^{-1}. These attributes lie between the battery and conventional capacitor. SCs also have an outstanding lifetime (duty cycle up to 1000,000 cycles) (Conway, 1999).

In the device setup shown in figure 2.2 each electrode-electrolyte interface represents a capacitor so that the complete cell can be considered as two capacitors in series. For a symmetrical capacitor (similar electrodes), the cell capacitance (C_{cell}), will, therefore, be:

$$\frac{1}{C_{cell}} = \frac{1}{C_1} + \frac{1}{C_2} \qquad \mathbf{1}$$

Where, C_1 and C_2 represent the capacitance of the first and second electrodes, respectively. The capacitance, measured in Farad (F), is defined as the ratio of total charge in Coulomb (Q) in each electrode to the potential difference (V) between the plates:

$$C = \frac{Q}{V} \qquad \mathbf{2}$$

The capacitance is also proportional to the surface area (A) of the plates and inversely proportional to the distance (d) between the plates multiplied by a permittivity constant ε_0 (8.8542×10^{-12} C^2 Nm^{-2}):

$$C = \frac{\varepsilon_0 A}{d} \qquad \mathbf{3}$$

Also, the double-layer capacitance at each electrode interface is given by:

$$C = \frac{\varepsilon A}{4\pi d} \quad \textbf{4}$$

Where **ε** is the dielectric constant of the electrical double-layer region, **A** the surface area (cm^2) of the electrode and **d** is the thickness of the electrical double-layer (cm). The stored energy of the capacitor in joules (J) is proportional to the capacitance (C) and voltage (V) square across the plates:

$$E = \frac{1}{2} C V^2 \quad \textbf{5}$$

It should be noted that the energy equation assumes that the initial voltage of the capacitor is zero. If the voltage is not zero, then the energy equation becomes:

$$E_1 - E_2 = \frac{1}{2} C ¿ \quad \textbf{)} \quad \textbf{6}$$

Where V_2 is the final voltage and V_1 is the initial voltage.

2.3 Ragone Plot of Energy Storage Devices

The Ragone plot below is a graph of power density against the energy density of various energy storage devices. It is shown from the plot that SCs occupy a region between the conventional capacitors and the batteries. The batteries and low-temperature fuel cells have a very high energy density range of 10 Wh kg^{-1} to 100 Wh kg^{-1} which shows that they store a high amount of energy but they have a low charge or discharge rate due to low power density. Conventional capacitors such as electrolytic capacitors have high power density greater than 10^6 W kg^{-1} but have low energy density.

For effective energy storage, SCs stores up to hundreds and thousands of energies than the conventional capacitor but could not match the energy density of mid to high-end of batteries and fuel cells. The current trend of research is to improve the energy density of SCs without compromising the power density.

Energy Density (Wh/kg)

Figure 2-1 Ragone plot of energy storage (Kötz & Carlen, 2000)

Table 2-1 *Comparison of the conventional capacitor, supercapacitor, and batteries* Yong Zhang et al (Li et al., 2010).

Properties	**Capacitor**	**Electrochemical Supercapacitor**	**Battery**
Discharge time	10^{-3} to 10^{-6} s	0.3-30 s	0.3-3 h
Charge time	10^{-3} to 10^{-6} s	0.3-30 s	1-5 h
Energy density (Wh/kg)	<0.1	1-10	10-100
Specific power (W/kg)	>10,000	≈1000	50-200
Cycle life	>500,000	>100,000	500-2000

2.4 the Working Principle of Supercapacitors

SCs use an "electric double-–layer" instead of a dielectric for charge storage. Their storage energy mechanism is by bulk movement and separation of charges. The electric double-layer is formed at the interface between the electrode and the electrolytes. SCs are also composed of a

separator that prevents contact between the negative and positive electrodes, two electrodes and electrolytes which could be aqueous or organic electrolytes. The electrode material could be carbon materials, mixed metal oxides or conducting polymers (Winter & Brodd, 2004). Various forms of carbon-based material used as an electrode for SCs are activated carbon, carbon nanotube, and carbon cloth.

SCs are charged when the ions in the electrolytes diffuse into the pores of the electrode of opposite charge and electric energy is stored as the voltage is applied.

They are discharged on the application of load when the accumulated ions are released from the electrode surfaces back into the electrolytes. There is no chemical reaction in SCs since a thin layer is formed by the movement of the ions. As a result, it has a very large charge-discharging life cycle (1,000,000 cycles). The high surface area of the electrode and thin electric double--layer gives SCs a high capacitance value (Li et al., 2010).

Figure 2-2 Typical configuration of supercapacitors (Li et al., 2010)

2.5 Advantages of Supercapacitor Technology

I. SCs have high cycle stability that is up to 1 000,000 cycles (Conway, 1999), at several degrees below zero they can be fully charged and discharged in seconds (Vuorilehto & Nuutinen, 2014).

II. They have almost linear voltage curves that enables very accurate state of charge (SoC) estimations (Vuorilehto & Nuutinen, 2014).

III. They have high power densities compared to that of batteries (Vuorilehto & Nuutinen, 2014).

IV. One of the major advantages of supercapacitors is that they can work at very low-temperature; at that temperature, the electrochemical batteries are ineffective (Vuorilehto & Nuutinen, 2014).

2.6 Applications of Supercapacitors

SCs deliver superior electrical performance in several applications because they resolve the shortcomings of lead-acid and lithium-ion batteries (Confidential, 2012).

Some of these applications are:

I. Starting of internal combustion engines (ICE): Since SCs have a high power density, low series resistance, and high cycle stability; they are used as a complementary source to batteries for starting internal combustion engines (Kroics, 2015). Thus, SCs make a substantial extension of battery life-span, reduce weight, volume and lowers the starting

time and energy (Stanca, Borza, Romanca, Paun, & Zamfir, 2010).

II. Electric Vehicle (EV) and Hybrid Electric Vehicle (HEV): SCs are used in combination with batteries in EVs or HEVs to enhance fuel reduction to about 20 to 60% by recovering their break energy (A Burke & Zhao, 2015). SCs are still essential as a power buffer for electric vehicles for large battery packs in order to recapture break energy by utilizing the currents that are beyond the battery limit, provide power acceleration beyond the power density of the battery and also provide secure power for steering, break and some other critical function if the battery fails.

III. Aviation: SCs are used in airliners like an Airbus 380 to power emergency actuators for doors and evacuation slides (Maxwell Technologies Ultracapacitors Regenerative Power).

IV. Military: SCs have important characteristics of low internal resistance as a result, they are used in applications that require short-term high currents like engines in submarines. The high specific power of SCs makes them suitable for phased array radar antennae, avionic display and instrumentation, military radio communications, and as a backup power for GPS-guided missiles and projectiles ("Supercapacitors for Military, Defense, Space, Isro, Spel, Capacitors, India's First Supercapacitor, Ultracapacitors,")

2.7 Storage Mechanism of Supercapacitors

SCs can be classified according to charged energy storage mechanisms and the active materials used. There are three broad classifications namely: electric double-layer supercapacitors (EDLCs), pseudo-supercapacitors, and hybrid supercapacitors as shown in **Figure 2-3** below.

Figure 2-3 Storage mechanism of supercapacitors (Al, Gualous, Omar, & Van, 2012)

2.7.1 Electric Double-layer Supercapacitors (EDLCs)

Electrochemical double-layer capacitors (EDLCs): They are SCs that store charge using non-faradaic or electrostatically, there is no charge transfer between the electrode and the electrolyte. There is no chemical change associated with EDLCs, as a result charge storage is reversible and high cyclic stability is achieved. They utilize an electrochemical double-layer of charge to store energy. EDLCs are composed of carbon-based electrodes (activated carbon, carbon nanotube, and carbon aerogel), an electrolyte, and a separator. On application of voltage, ions in the electrolytes migrate through the separator to the pores of the opposite electrode charge. (Andrew Burke, 2000) (Conway, 1999)

In EDLCs, electrostatic storage is obtained by charge separation in a Helmholtz double-layer at the interface between the carbon-based electrode and the electrolyte. It has a separation distance of 0.3 nm to 0.8 nm in the double-layer which is static in origin (Namisnyk, Namisnyk, Zhu, & Zhu,). Carbon-based materials are mostly used in the electrode of EDLCs because of their desirable chemical and physical properties like controllable porosity, availability, ease of processability, and relatively inert electrochemistry. These carbon-based materials appear in various forms like powder, fibers, aerogels, composite, sheets, tubes and monoliths. (Zhang & Zhao, 2009).

2.7.2 Pseudocapacitors

They are another classification of SCs where electrical energy is stored faradically. There is reaction associated with the transfer of electron charge between the electrode and electrolyte (Garthwaite, 2011). Pseudocapacitors can achieve greater capacitance and energy density more than EDLCs due to the faradaic processes. Pseudocapacitors use conducting polymers and metal oxide electrode material to store charge (Ellenbogen, 2006). In pseudocapacitors, there is a linear relationship between the charge stored and applied voltage (Brezesinski, Wang, Tolbert, & Dunn, 2010).

2.7.3 Hybrid Capacitors

Hybrid capacitors are the class of supercapacitors that utilize both faradic and non-faradic mechanisms to store electric charge. Hybrid capacitors achieve higher power densities than EDLCs and also overcome the limitation of cycling instability and high cost that is associated with pseudocapacitors. Hybrid capacitors utilize the strength of both EDLCs and pseudocapacitors while overcoming their shortcomings. Hybrid Capacitors are distinguished by their types of electrodes and can be distinguished into, asymmetric, and battery-type (Ellenbogen, 2006).

2.7.3.1 Asymmetric Hybrid

An asymmetric hybrid utilizes both faradaic and non-faradaic mechanisms in storing charges. This is achieved by coupling a carbon-based electrode (non-faradaic or electrostatic charge storage) with the pseudo-capacitive electrode (faradaic), which can serve as either an anode or cathode in the system. One of the most common types of this configuration is activated carbon/MnO2 SCs (Rolda et al., 2014). The conducting polymer Pseudocapacitors suffer a setback due to the lack of effective negatively charged conducting polymer materials. The asymmetric hybrid system solves this problem by coupling with the negatively charged activated carbon electrode. An asymmetric hybrid capacitor reduces the tradeoff to obtain high power and energy densities than EDLCs (Ellenbogen, 2006).

2.7.3.2 Battery-Type Hybrid

The battery-type hybrid is also an asymmetric process that combines a rechargeable battery-type reaction with a capacitive electrode (Rolda et al., 2014). Batteries are known for their high energy densities while SCs have high power density and a long cyclic life. Like the asymmetric hybrid, battery-type hybrid couples the electrode of SCs and that of a battery in order to achieve both qualities of batteries and SC in a single device. The current research on a battery-type hybrid focuses on coupling nickel hydroxide, lead dioxide, and LTO (Li4Ti5O12) electrode and activated carbon as the second electrode. Battery-type hybrids bridge the gap between SCs and batteries (Ellenbogen, 2006).

2.8 Materials for Electrodes of SCs

The materials for SCs are selected based on the type of capacitance to be utilized. The capacitance could be double-layer, pseudocapacitance and hybrid capacitance which is the combination of a double-layer and pseudocapacitance. Materials for electrodes are categorized into three: carbon-based, transition metal oxides, and conductive polymers (Ellenbogen, 2006).

2.8.1 Carbon-based Material

Carbon-based materials are mostly used as an electrode material for supercapacitor electrodes because they are cheap, readily available, and have a high specific surface area. The carbon-based materials are: activated carbon, graphite, carbon aerogels, AC fiber cloth, carbon nanotube, graphene and mesoporous carbon.

2.8.1 Activated Carbon (AC)

AC is mostly used as an EDLCs electrode material because it is cheap, has a high surface area and variable pore size which is dependent on activation processes (Zhang & Zhao, 2009). There is an empirical relationship between the pore size, energy density, and power density. The higher the pore volume, the higher the power density and the lower the energy density (Ellenbogen, 2006). In theory, an increase in the specific surface area of the AC increases the capacitance of the EDLCs. The ionic conductivity which defined the ionic mobility migration inside the pores is determined by the porous structure of the activated carbon. (E. Frackowiak, 2001). The porous structure of activated carbon is classified into micropores, mesopores, and macropores (Ellenbogen, 2006).

2.8.1.1 Carbon Aerosol

Carbon aerosols are one of the outstanding materials for EDLCs due to their high electrical conductivity and their large specific area. They also consist of carbon nanoparticles of the three-dimensional network (Li et al., 2010). It can be obtained by pyrolysis of resorcinol-formaldehyde aerogels. Experimental analysis shows that a volumetric capacitance of 46 F/cm^3 was obtained for a sample of density 800 kg/m^3 which is pyrolysis at 800 ^oC (Fischer, Saliger, Bock, Petricevic, & Fricke, 1997). A carbon aerosol has lower equivalent series resistance (ESR) than activated carbon hence, higher power density (Ellenbogen, 2006).

2.8.1.2 Graphene-Based Supercapacitor

The graphene-based materials are promising for applications in supercapacitors and other energy storage devices due to their intriguing properties, *i.e.*, highly tunable surface area (2675 m^2 g^{-1}), outstanding electrical conductivity, good chemical stability and excellent mechanical behavior (Ke & Wang, 2016). It is also very light because it is a single atomic layer of graphite and ecologically friendly. Scientists were able to create a supercapacitor that could store up to 150 F/g while graphene-based supercapacitors store 550 F/g as their theoretical upper limit. This is quite an interesting result when compared with the current technology.

2.8.1.3 Carbon Nanotubes

Carbon nanotubes (CNTs) have emerged as an important electrode material for electrochemical double-layer capacitors because of their properties of open and accessible network of mesopores, high specific surface area, and high charge transport process (Elizabeth F. Rangel & Carvalho, 2017). Although the surface area of CNTs is not as high as that of activated carbon, they allow effective charge distribution that utilizes most of the available surface area due to the interconnection of the mesopores. As a result, carbon nanotubes achieve a reasonable capacitance that is comparable to those of activated carbons. The ease at which electrolytes ions diffuse into the mesoporous network of CNTs makes their equivalent series resistance (ESR) lower than activated carbon (Li et al., 2010). CNTs are two-dimensional graphene sheets with cylindrical nano-structure which is made of hexagonally oriented carbon atoms. Their diameter and lengths are in the nanometer range and micro-scale respectively. There are two major classifications of CNTs, i.e., single wall carbon nanotubes (SWCNTs) and multiple wall carbon nanotubes (MWCNTs). SWCNTs are formed by wrapping a single sheet of a one-atom-thick layer of graphene in cylindrical form. The indices signify the number of a unit vector along the hexagonal lattice of graphene.

While MWCNTs are composed of many rollers of the graphene sheet. Like activated carbon, CNTs can also be activated in order to increase the BET surface area and pore volume by 3 times and 5 times respectively (Li et al., 2010).

Fig 2-4 Carbon nanotubes (X. Wang et al., 2009)

Table 2-2*: Summary of carbon-based electrode materials investigated by Yong Zhang et al (Li et al., 2010)*

Carbon-based	Electrolyte	Working voltage (V)	SC (F/g)
Activated carbon	1 M Et4NBF4+PC	1.5	40
Graphite	1 M Et4NBF4+PC	3.0	12
Carbon aerogels	1.5M Et3MeNBF4+PC	3.0	160
AC fiber cloth	6 M/L KOH	1.0	208
Sing-walled CNTs	EMITFSI	2.3	50
Multi-walled CNTs	1.96 M TEMABF4+PC	2.5	13
Mesoporous carbon	30 wt% KOH	0.9	180

2.8.2 Conducting Polymers (CPs)

CPs are used as an electrode material due to their fast-redox reaction and high conductivity. They are cheap, have high capacitance and low equivalent series resistance (ESR) compared to carbon-based electrode materials that are used for double-layer capacitors. CPs have a high power capability than inorganic battery materials. The shortcomings of CPs as electrode materials are as follows; they have poor charging and discharging cycles, and they also swell and contract during the electrochemical process (Snook, Kao, & Best, 2011). The most commonly used CPs for SCs applications are Polythiophene (PTH), Poly (p-phenylene vinylene) (PPV), Polyaniline (PANI), Polypyrrole (PPy), and Poly (3,4-ethylene dioxythiophene) (PEDOT). They can be synthesized either by chemical or electrochemical oxidation of the monomer. The conducting polymers are classified into two charging processes namely: P-doped with anions when oxidized and n-doped with cations when reduced (Li et al., 2010).

Table 2-3 Investigation of conducting polymer electrode material *Yong Zhan et al (cited in Li et al., 2010).*

Conductive polymers	Electrolyte	Working voltage (V)	SC (F/g)
Poly(3-ethylthiophene)	PYR14TFSI	3.6	25
Polypyrrole/AC	0.5 M Pyrrole/β-NSA	0.9	345
PANI/MnO2	0.1 M Na2SO4	1.2	715
PANI/AC	6 M KOH	0.9	588

2.8.3 Transition Metal Oxides (TMOs)

TMOs are known for their high pseudocapacitance as a result of their multiple valence states which is not obtainable in carbon materials. Generally, TMO metals are very attractive in the field of energy storage and conversion because of their mechanical and electronic properties. TMOs are classified into RuO2, IrO2, MnO2, NiO, Co3O4, NiCo2O4. The noble TMOs have higher capacitance, are cheaper and more environmentally friendly than the base transition metal (Wu, Zhu, Ji, & Banks, 2016). TMOs are also an attractive material used in electrodes for electrochemical capacitors because of their high intrinsic capacitance. Among all the transition metals, ruthenium oxide (RuO2) is the most outstanding due to its high conductivity, high specific capacitance, good electrochemical reversibility and long cycle life (Li et al., 2010).

Table 2-4: Investigation of metal oxide material *(Li et al., 2010)*

Metal oxide	Electrolyte	Working voltage (V)	SC (F/g)
$RuO_2 \cdot H_2O$	0.5 M H_2SO_4	1.0	650
$H_{0.2}RuO_{2.1} \cdot nH_2O$	0.5 M H_2SO_4	1.2	390
MnO_2	0.5 M K_2SO_4	0.8	261
$Ni(OH)_2$	3% KOH	0.8	578
Mo_2N/Ta_2O_5	3.5 mol/L H_2SO_4	0.8	106
$MnFe_2O_4$	1 M $LiPF_6$+EC/EMC	2.5	126
TiN	1 M KOH	0.2	238
V_2O	2 M KCl	0.7	262

2.8.4 Composite

Composite electrodes are formed by integrating carbon-based electrodes with either polymers or metal oxide materials in order to incorporate both chemical and physical charge mechanisms in a single electrode.

The carbon-based material increases the electrode surface area thereby increasing the pseudo-capacitive materials and electrolyte contact (Ellenbogen, 2006). Composite electrode mechanism increases the power density without compromising on the energy density (Li et al., 2010). A composite of Nickel-manganese oxides/multiwall carbon nanotubes/poly (3,4-ethylene dioxythiophene) (NMO/MWCNTs/PEDOT) nanocomposite was prepared by a chemical oxidation method as a SC electrode and the result was an excellent (Kiamahalle, Cheng, Sata, Buniran, & Zein, 2011).

2.9 Electrolytes

The performance of a SC is not only affected by the electrode material but also the choice of electrolytes. An electrolyte is the composition of electrolytic salt and solvent which provides ionic conductivity and also facilitates the electron migration on cell electrodes. The electrolytes enhance the formation of the electrochemical double-layer and the reversible redox process during charge storage in EDLC and in pseudocapacitors respectively (Zhong et al., 2015). The internal resistance of SC, the cycle life, and the power/energy density are also determined by the conductivity of the electrolytes, the interaction between the electrolytes, the electrode material and the voltage window of the electrolytes. Equation 1 and 2 above show that the power and energy density are influenced by the operational cell voltage of electrochemical SCs which is determined by the electrochemical stable potential window.

SC electrolytes can be classified as solid/ quasi-solid-state electrolytes and liquid electrolytes. Liquid electrolytes are grouped into aqueous electrolytes, organic electrolytes, and ionic liquids while solid electrolytes are grouped into organic electrolytes and inorganic electrolytes (ESPW) (Li et al., 2010).

2.9.1 Liquid Electrolytes

Liquid electrolytes are grouped into aqueous electrolytes, organic electrolytes, and ionic liquids.

2.9.1.1 Aqueous Electrolytes

Aqueous electrolytes are the most used liquid electrolytes in electrochemical SC due to their high conductivity which is greater than that of organic and ionic liquid electrolytes. The high conductivity of aqueous electrolytes increases the power density of ESs by lowering equivalent series resistance (ESR) (Li et al., 2010). Aqueous electrolytes are also cheap and very easy to handle as electrolytes, unlike organic and ionic liquid electrolytes that need special purification under a controlled atmosphere to avoid contamination by moistures.

The major shortcoming of aqueous electrolytes is their short voltage window which leads to low energy density SCs (Zhong et al., 2015). The criteria for selection of aqueous electrolytes are the mobility of the ions, the size of bare and hydrated ions and cations. These criteria affect both capacitance value and ionic conductivity. Aqueous electrolytes are further grouped into acidic alkaline and neutral solutions like H2SO4, KOH and Na2SO4 respectively (Zhong et al., 2015).

2.9.1.2 Organic Electrolytes

Unlike aqueous electrolytes, organic electrolyte-based electrochemical SCs have a high operational voltage window in the range of 2.5V to 2.8V which increases both the energy densities and the power densities significantly (Li et al., 2010). The high voltage window of organic electrolyte-based SCs is due to their higher decomposition limit of the electrolytes. Also, due to the large organic molecules, organic electrolytes have a greater pore size (15-20 Å).

Although organic electrolytes have a higher resistivity (20-60 Ω) than aqueous electrolytes which reduce their power densities, this effect is compensated by the higher voltage window of the organic electrolytes. Despite these aforementioned advantages, some of the issues associated with organic electrolyte-based SCs are lower conductivity, high cost, smaller specific capacitance, flammability, toxicity, and volatility. They also require complex purification and assembling in a controlled environment to eliminate some impurities like moisture in order to avoid performance degradation and the problem of self-discharge (Zhong et al., 2015).

2.9.1.3 Ionic Liquid Electrolytes

Ionic liquid electrolytes are salt composed of ions with a low melting point which is less than 100 °C (Kim & Ahn, 2015). Ionic liquid electrolytes are mostly composed of both asymmetric organic cation and an inorganic or organic anion which have a low melting point as a result of this unique combination. Ionic liquid has many advantages as electrolytes for electrochemical SC application like low vapor pressure, wide electrochemical window, high ionic conductivity and high thermal stability (Li et al., 2010).

The physical and chemical properties of the ionic liquid are tunable as a result of many variations of cations and anions combination. This attribute is very important for SC electrolytes because the compositions of the electrolytes can be optimized or modified in accordance with required SC performance like the working temperature range, and operative cell voltage (Freemantle, 1998). Some of the ionic liquids (ILs) cations used in SCs are sulfonium, phosphonium, pyrrolidinium, ammonium, Imidazolium, and pyrrolidinium while some of the anions are dicyanamide (DCA), tetrafluoroborate (BF4), bis(trifluoromethane sulfonyl)imide (TFSI), and hexafluorophosphate (PF6). From the listed ILs cations, pyrrolidinium-based ILs have larger potential windows. While the imidazolium-based ILs can deliver higher ionic conductivity.

Despite the several advantages of ILs, they have some downside as SCs electrolytes such as low ionic conductivity as high viscosity and high cost (Zhong et al., 2015).

2.9.2 Solid/quasi-solid-state electrolytes

Solid-state based electrolytes have become an important research area because of high growth of power for portable electronics and miniaturization of electronic devices. Unlike most liquid based electrolytes, solid-state electrolytes can serve both ionic conducting media and electrode separators. Solid-state electrolytes make the packaging and fabrication processes of SCs very simple and eliminate the risk of liquid-leakage. The two major types of solid-state electrolytes used for fabrications of SCs are polymer-based electrolytes and inorganic solid-based electrolytes like ceramic (Zhong et al., 2015).

2.9.2.1 Polymer-based solid electrolytes

Polymer-based solid electrolytes are classified into three major groups: The gel polymer electrolytes (GPE), and the solid polymer electrolytes

The gel polymer electrolytes (GPE) are also known as quasi-solid-state electrolytes due to the presence of liquid phase. The composition of GPE is polymer hosts and an aqueous electrolyte like H2SO4 or a solution of conducting salt in a solvent. In GPE, the polymer is the matrix which can be swollen by the solvent while ions migrate to the solvent instead of the polymer phase.

The advantage of GPEs are their high conductivity due to the presence of liquid phase which is greater than the conductivity of solid polymer electrolytes. The disadvantages of GPEs are a low mechanical strength which can cause internal short circuit and a narrow operating temperature range especially when water is used as the solvent. Some of the polymer matrix used in GPEs are poly (vinyl alcohol) (PVA), poly (acrylic acid) (PAA), potassium polyacrylate (PAAK), poly (ethyl oxide) (PEO), poly- (methyl methacrylate) (PMMA), and poly (ether ether ketone) (PEEK).

The solid polymer electrolyte (SPE) is also known as a dry electrolyte which is composed of a polymer like PEO and a salt like LiCl. The migration of salt ions through the polymer provides the ionic conductivity of SPE (Zhong et al., 2015).

2.9.2.2 Inorganic solid-state electrolytes

Inorganic solid-state electrolytes for SCs are generally mechanically robust and thermally stable. An example of inorganic solid electrolytes is Li2S–P2S5 glass-ceramic which is used both as an ion conductor and as a separator for all solid-state SCs. In order to improve the interfacial contact between the electrode material and the electrolytes, CNT is incorporated into the electrode material as a specific capacitance and the SC will be enhanced (Zhong et al., 2015).

2.10 Soot

Soot is a mass of impure carbon which is formed as a result of incomplete combustion of hydrocarbon or the conversion of hydrocarbon fuel molecules into carbonaceous agglomerates (Omidvarborna, Kumar, & Kim, 2015). It is mostly formed by fuel combustion in engines and has a density of 1.84701 g/cm3 (Choi, Hamins, Rushmeier, & Kashiwagi, 1994). Soot nucleates at an elevated temperature from the vapor phase to a solid phase in fuel-rich regions (Kumar et al., 2011). It is a large particle black carbon/smoke present in exhaust gases. The soot size is sub-micron and has a necklace-like shape that agglomerates under scanning electron microscope. The initially formed soot has the highest content of hydrogen that is, the C/H ratio is almost one but the carbon fraction increases as the soot matures.

There are also traces of some elements such as iron, silicon, chromium, phosphorus, calcium, and zinc present in emitted soot from a diesel engine (Omidvarborna et al., 2015).

2.10.1 Mechanism of Soot formation

According to Tree and Svensson, the mechanism of soot formation involves five steps which are pyrolysis, nucleation, surface growth, coalescence, and agglomeration. It is as shown in the figure below.

Figure 2- 5 Mechanism of soot formation (Tree & Svensson, 2007)

Pyrolysis: is thermochemical decomposition of organic material (Fuel) in the absence of oxygen or any other halogens to produce precursors with polyaromatic hydrocarbons PAH-like Acetylene (C2H2) which is the onset of soot formation (Tree & Svensson, 2007).

Nucleation: Nucleation is the next step in soot formation which is the inception of heavy PAH molecules to form particles which are the nascent soot. This nascent soot has an approximately 2000 atomic mass unit (amu) (Haynes & Wagner, 1981). Its effective diameter as detected by a high resolution transmission electron microscope is about 1.5 nm. Nucleation commences at lower amu of 300-700 (Frenklach & Ebert, 1988).

Surface growth: is the mechanism by which soot particle masses grow by the addition of gas species like acetylene and PAH molecules/radicals. The surface reaction of soot particles and the gas species is through hydrogen abstraction and carbon addition (HACA) (Omidvarborna et al., 2015).

Coalescence: It is the combination of two or more particles to form a larger particle. It is also known as coagulation and it proceeds almost immediately after soot particle formation. This process increases the particle size, decreases the number of particles, while the mass of the soot present remains the same (Omidvarborna et al., 2015).

Agglomeration: Agglomeration is the last stage of soot formation which occurs when primary particles stick to each other to form chain-like aggregates. This is majorly found in the exhaust of a diesel engine (Omidvarborna et al., 2015).

CHAPTER THREE

3.0 Experimental Procedure

3.1 Purification of Sample (soot)

Soot deposit from an automobile was collected and leached with hydrochloric acid (H2SO4) to remove oil content and minerals in the soot. It was further washed with distilled water and dried in an oven at 70 ^{o}C for 12 hours.

3.1.2 Carbon Activation

Carbon activation is the processing of carbonaceous material to have small low-volume pores that increase the surface to adsorption properties. Activated carbon has an excellent surface area per unit volume, a pore size distribution within three pore regions: the micropore, mesopore, and macrospore regions. The gas adsorption experiment shows that one gram of carbon has a surface area in excess of 3,000 m^2 (Dillon, Wilton, Barlow, & Watson, 1989).

3.1.2.1 Soot Activation Procedure

- The sample is divided into three (sample1, sample2 and sample3), each mixed with KHCO3 (activating reagent) at different ratios; 1:10, 1:8, and 1:6 respectively, and at the same temperature of 700 ^{o}C.

After mixing all the samples with the activating reagent, the mixture was placed inside the horizontal reactor which was heated inside a furnace. An inert gas (Nitrogen) was passed through the reactor to make the environment inert for activation as shown in the setup below.

Figure3-1 Carbon activation setup

3.2 ELECTROCHEMICAL EXPERIMENT

The electrochemical experiment used was the three-electrode cell setup which is shown in the figure below. The three electrodes used were working electrode (WE), a counter electrode (CE), and a reference electrode (RE). Gamry potentiostat was used for the electrochemical experiment.

The counter electrode also known as an auxiliary electrode is made of inert material like graphite, platinum (Pt), gold (AU) and glassy carbon. It did not participate in the chemical reaction but was only used to close the current circuit in the electrochemical cell. The total surface area of the CE is always higher than the area of WE so that kinetics of the electrochemical process under investigation would not be affected by current flows between the WE and the CE. Graphite material was used as the counter electrode.

The reference electrode was a stable electrode with well-known electrode potential, used as a point of reference in the electrochemical experiment for the potential control and measurement.

The redox system with a constant concentration of each member of the redox reaction was employed in order to achieve high stability of the reference electrode. The current flow through the reference electrode was approximately equal to zero which was achieved by the use of CE that closes the current circuit in the cell and with a very high impedance greater than 100 Gohms on the electrometer.

The WE is the electrode in an electrochemical system which was under investigation. The reaction of interest occurs at the WE. Some of the common WE are made of inert materials like AU, Ag, carbon materials and film electrode. Activated soot was used as the working in this research.

3.3 PREPARATION OF WORKING ELECTRODE

80% of activated soot was mixed with 10% acetylene black and 10% of polyvinylidene difluoride (PVDF) binder with some drops of a liquid N-Methylpyrrolidone (NMP) to dissolve the binder and the mixture was ground inside a ceramic mortar. The acetylene black improved the conductance of exhaust carbonaceous soot. The PVDF improved the electrochemical stability, mechanical strength and capacitive characteristics of the electrode material (Hou, Huang, Lin, & Wang, 2012). The homogenous mixture was coated on a carbon paper of surface area $1cm^2$ as the WE material and one molar sodium trioxonitrate iv (1M $NaNO_3$) was used as the electrolyte.

3.4 EXPERIMENT SET -UP

A three-electrode cell is the electrochemical setup used for the electrochemistry as shown in **Figure3-2** below. In this setup, the current flowed between the CE and WE while the potential difference was controlled between them. The potential difference was measured between the RE and WE (connected together with the sense electrode). The WE was kept at a fixed stable potential by controlling the polarization of the CE, thereby controlling the potential difference between WE and RE at all time.

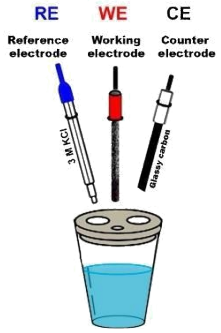

Figure 3-2 The three-electrode cell setup

3.5 Characterization

3.5.1 Brunauer–Emmett–Teller (BET) Experiment

BET is a gas adsorption experiment which shows the capacity of a solid surface to adsorb gas molecules. It is an analytical technique for measurement of the specific surface area of a material (Brunauer, Emmett, & Teller, 1938). The BET experiment was used to study the system of multilayer adsorption which utilizes probing gases that do not react chemically to adsorbates material surface and measure the specific surface area. The most common gaseous adsorbates used for BET experiment is nitrogen which is conducted at boiling temperature of N_2 (77k). Other gases used for BET experiment are argon, carbon dioxide, and water (Hanaor, Ghadiri, Chrzanowski, & Gan, 2014).

3.5.2 Adsorption Isotherms

Adsorption isotherm is the most common method of describing adsorption phenomena. It is used for the determination of internal surface area and pore volume of activated carbon and it is a plot of the amount of adsorbed molecules (x/m mmol/g) against the relative pressure of adsorptive (p/p0) at equilibrium and constant temperature.

Adsorption isotherm has six classifications according to IUPAC (International Union of Pure and Applied Chemistry). It is shown in **Figure 3-3**

Figure 3-3 IUPAC's classification of the adsorption isotherms (Shabanzadeh, 2012)

Type-1 demonstrates adsorption isotherms that attain a maximum value of adsorption without inflections and these isotherms are characteristics of carbons that contain only micropores. The gradient of this isotherm has a relative pressure (P/Po) from zero to about 0.05 which shows the dimension of micropores. The steep initial region is as a result of strong adsorption and the steeper the gradient the narrower the micropores (Shabanzadeh, 2012).

Type-II adsorption isotherms describe the polymolecular adsorption in non-porous or microporous adsorbents.

Type III refers to low energy adsorbent-adsorbate interaction for non-porous sorbents.

Type IV is similar to type II but adsorption takes place in the mesopores instead of the open surface at relatively high pressures and it is referred to as porous adsorbents.

Hysteresis is an indication of capillary condensation of mesopores and macrospores just like activated carbon.

BET and BJH (Barrett-Joyner-Halenda) models are applicable here.

Type -V refers to low energy adsorption isotherms of homogeneous solid surface, posed in mesopores. It does not require the BET model. Like type IV, it is referred to as porous adsorbents.

Type-VI isotherms refer to the characteristic of a non-porous adsorbent which has an extremely homogeneous surface (Shabanzadeh, 2012).

3.6 Scanning Electron Microscopy (SEM)

Scanning electron microscope (SEM) was used to produce the images/morphology of the samples by scanning the surface with a high-energy beam of electrons. There was an interaction between the electrons and the atoms of the sample that produced several signals about morphology and the composition of the sample (McMullan, 2006).

Operation of scanning electron microscopy (SEM)

Figure 3-4 Operation of scanning electron microscopy (SEM) (Ballantine et al., 1997)

The electron source in SEM is forced in a vacuum into a fine probe which is rastered over the surface of the specimen or sample. When the electron penetrates the surface of the specimen, the

interaction between the electron beams with the atoms of the sample at several points generate a signal used by the SEM to produce an image. Some fractions of the signal are collected by appropriate detectors, its output is used to modulate the brightness of the cathode ray tube (CRT) whose x and y input synchronizes with x-y voltages restering the electron beam thereby producing an image on CRT. The various signals used by the SEM to produce images are secondary electrons (SE), characteristic X-rays, reflected or back-scattered electrons (BSE) and light (cathodoluminescence) (CL), absorbed current (specimen current) and transmitted electrons (Ballantine et al., 1997).

3.7 Raman Spectroscopy

Raman spectroscopy is a nondestructive test that was used to show the chemical structure/phase, molecular interactions, and crystallinity of the sample. It provided the structural fingerprint by which molecules can be identified.

This technique depends on inelastic scattering, or Raman scattering, of monochromatic light usually from a laser in the visible, near infrared or near ultraviolet range. Inelastic or Raman scattering shows that the photon in monochromatic light changes upon interaction with the sample. After the absorption of the photons of the laser light, the sample reemits the photons and the photon's frequency is shifted up or down with respect to the original monochromatic frequency which is known as the Raman effect. The shift in the frequency gives the information about vibrational, rotational and other low-frequency transition in molecules.

Raman spectroscopy can be used to study gaseous liquid and solid samples. When incident photons from a laser beam illuminate a sample, if the initial state and the frequency of the emitted photon are the same as the incident, Rayleigh scattering (elastic scattering) occurs. If the final state has higher energy (frequency) than the initial state, the scattered photon will shift to a lower frequency /energy so that the total energy will remain constant. This shift in frequency is known as a Stokes shift or downshift.

Anti-stoke shift occurs when the final state has a lower energy than the initial state so that the scattered photon will be shifted to a higher frequency (Gardiner, 1989).

3-5 Energy-level diagram showing the states involved in Raman spectra *(Gardiner, 1989)*

3.8 Fourier-transform Infrared Spectroscopy (FTIR)

FTIR is a nondestructive test that is used to obtain the chemical bond of a material or thin film. When infrared radiation (IR) is passed through a sample, some IR is absorbed while some are transmitted. FTIR creates a molecular fingerprint of the sample which characterizes the molecular absorption and transmission. FTIR determines the change of IR as a function of frequency or wave length (Brault, 1996).

CHAPTER FOUR

4.0 Result and Discussion

4.1 FTIR Experiment

Figure 4-1 shows FTIR spectra of pristine (pure soot) and all the activated samples at a wave number range of 500-4000 cm^{-1}. Sample 1 and sample 3 have a similar vibrating peak while pristine and sample 2 have a similar vibrating peak as shown in the figure with a dotted line. The peak 1408 cm^{-1} is assigned to medium O-H bending vibration of carboxylic acid as by-product. The peak 1644 cm^{-1} is assigned to C=C stretching vibration of alkene disubstituted (cis) while the peak 3510 cm^{-1} is assigned to strong broad O-H stretching vibration and it is intermoleculary bounded.

Figure 4-1 FTIR spectra of pristine, sample1 sample 2 and sample 3

4.2 Raman Spectroscopy

Figure 4-2 (**a**) shows the Raman spectra of a pure soot, it consists of both D-band at ~1350cm^{-1} and G-band at ~1580cm^{-1}. The Raman signals arise as a result of lattice vibrations (phonons) of soot which are very sensitive to the degrees of structural disorder or defeat in a graphite material (Bokobza, Bruneel, & Couzi, 2014). The D-band(defeat) indicates that the disordered structure of the soot results in resonance Raman spectra while the G-band indicates the stretching of the C-C bond which is common to all sp^2 carbon system (Dresselhaus, Jorio, Hofmann, Dresselhaus, & Saito, 2010). The Raman spectra in **Figure 4-2** (**b**) show only structural disorder (D-band) of the graphite material without the D-band. **Figures 4-2 c** and **4-2 d** shows both D-band and G-band in which the D-band is of higher intensity than the G-band.

Figure 4-2 Raman spectra of samples (a) pure soot (pristine), (b) sample 1, (c) sample 2: and (d) sample 3

4.3 Scanning Electron Microscope (SEM) Experiment

The SEM micrograph of all the samples at both low and high magnification is very porous, rough, and uneven which is an indication of good adsorption properties. Thus, it is suitable for an electrode of supercapacitors.

h

Figure 4-3 SEM images of the samples (a, b) SEM image of sample 1 at different magnifications (c, d) high and low magnifications of sample 2, (e, f) high and low magnification SEM image of sample 3.

4.4 BET Analysis

After the preparation of the samples, all the samples were optimized at a temperature of 700°C and the BET specific surface area (SSA), meso–pore volume and micro–pore volume was tabulated in **Table 4-1** below. The results show that sample two (2) has the highest specific surface area (SSA) and meso–pore volume with the least pore diameter than the other samples. This implies that sample two (2) has a higher adsorption and desorption rate, therefore it has a superior capacitance electrode material compared to the other samples (Maryam, Suriani, Shamsudin, & Rusop Mahmood, 2012).

Table 4-1 BET results

	Sample 1	Sample 2	Sample 3
BET specific surface area (SSA)	11.5309 m^2/g	61.851 m^2/g	37.88 m^2/g
Mero pore volume	0.0022 cm^3/g	0.007 cm^3/g	0.0033 cm^3/g
Pore diameter	46.7 A^o	48.4 A^o	62.8 A^o

Figure 4-4b compares the nitrogen adsorption–desorption isotherm of the three samples. It shows that sample 2 and sample 3 belong to isotherms IV of IUPAC classification that refer to adsorption isotherms in mesopores. The hysteresis is an indication of capillary condensation in mesopores and macrospores. Sample 1 belongs to III of IUPAC classification which refers to low energy adsorbent-adsorbate interaction for non-porous sorbents. It demonstrates that the amount of adsorbed nitrogen for the sample 1 is 0.4179 cm^3/g is significantly lower than sample 2 and sample 3 which are 2.322 cm^3/g and 2.0287 cm^3/g respectively.

Figure 4-4 (a) Nitrogen adsorption–desorption Isotherm (b) pore size distribution of the three samples

4.5 Electrochemical Data

The electrochemical behavior of the samples was characterized by electrochemical impedance spectroscopy (EIS), cyclic voltammetry (CV), and charge-discharge (CD) using the three-electrode electrochemical setup. The electrode of each sample was probed in a 1.0 M $NaNO_3$ aqueous electrolyte. The CV was used to determine the surface reaction of active material during different scan rates. **Figures 4-5(a)**, **4-6(a)** and **4-7(a)** show the CV calve of sample1, sample 2 and sample 3 respectively at a scan rate of 5 to 50 mV^{-1}. The CV curve for all the samples increases in current with an increase in the scan rate. The quasi-rectangular CV curves indicate the electrical double-layer capacitor (EDLC) behavior of the samples. **Figure 4-8(a)** compares the CV curve of all the three samples and it shows that sample 2 has the highest CV area which indicates that it exhibits the best capacitive behavior when compared to the other two samples. Sample 3 has a better capacitive behavior than sample1 by virtue of the higher CV area.

Figures **4-5**(**b**), **4-6**(**b**) and **4-7**(**b**) show the galvanostatic charge-discharge curve for samples 1-3 respectively, and at different current densities from 0.5 - 5.0 Ag^{-1} on a potential range of -0.8 and 0 V. It is observed that CD curves were near linear and symmetrical which is as a result of O-H functional group as shown in the FTIR result. A negligible voltage drop is observed in the CD curve which indicates a low internal resistance of the electrode material. The CD curve is also used to calculate the specific capacitance by using the following equation:

$$c = \frac{It}{m \nabla v} 4-1$$

$$c = \frac{It}{m \nabla v} 4-1$$

$$c = \frac{It}{m \nabla v} 4-1$$

Where t is discharge time (s), I current (A), ∇v voltage range (V) m mass of active material (g).

Figures 4-6(**d**) and **4-7**(**d**) show the plot of specific capacitance against current density for sample1-3 respectively. The specific capacitance of 42.5 F g^{-1}, 85. F g^{-1} and 83.25 F g^{-1} were obtained at a current density of 0.5 $Ag^{-1.}$ These plots imply that specific capacitance increases with a decrease in the current density.

Figure 4-8d compares the specific capacitance of the three sample electrodes and it indicates that sample 2 is the best capacitance electrode material because it has the highest capacitance value.

Figures 4-5(**c**), **4-6**(**c**) and **4-7**(**c**) show the EIS of samples 1-3 respectively, which is the representation of both real and imaginary parts of the impedance of the material electrodes. The plot in **Figure 4-5**(**c**) is composed of two regions: the partial semi-circle in the high-frequency region and a tilted line in the low-frequency region. The partial semi-circle is an indication of the charge transfer processes which take place at the interface between the electrode and electrolyte, while the tilted line is an indication of the Warburg resistance which is mainly associated with a double-layer capacitance (Gamby, Taberna, Simon, Fauvarque, & Chesneau, 2001). The partial semi-circle occurs as a result of dispersion effect.

The ESR of sample 1 is the intercept at a high-frequency region and is equivalent to 68.85 ohms (Bai, Liu, Sun, & Gao, 2016).

Figures 4-7c and **4-8c** have no partial semi-circle in the high-frequency region which is an indication of very low charge transfer resistance (L. Wang, Li, Guo, Yan, & Tay, 2014). **Figure 4-9c** demonstrates the comparison of the three samples. It shows that sample 2 has the shortest diffusion length which corresponds to smallest resistance. The smallest resistance of sample 2 also indicates that it is a superior capacitance material compared to the other two samples.

Figure 4-5 Electrochemical analysis of sample 1

Figure 4-5(**a**) CV at different scan rates ranging from 5–50 mV^{-1}; (b) galvanostatic charge/discharge at current densities of 0.5- 4 Ag^{-1}; (c) Nyquist plot (d) specific capacitance at different current densities (CD curve).

(a) CV at different scan rates ranging from 5–50 mV^{-1}; (b) galvanostatic charge/discharge at current densities of 0.5- 4 Ag^{-1}; (c) Nyquist plot (d) specific capacitance at different current densities (CD curve).

Figure 4-7 Electrochemical analysis of sample 3

(a) CV at different scan rates ranging from 5–50 mV^{-1}; (b) galvanostatic charge/discharge at current densities of 0.5- 4 Ag^{-1}; (c) Nyquist plot (d) specific capacitance at different current densities (CD curve).

Figure 4-8 Electrochemical analysis comparing the three samples

(a) CV at different scan rates ranging from 5–50 mV^{-1}; (b) galvanostatic charge/discharge at current densities of 0.5- 4 Ag^{-1}; (c) Nyquist plot (d) specific capacitance at different current densities (CD curve).

CHAPTER FIVE

5.1 Conclusions and Recommendations

There is need to improve the performance of electrochemical supercapacitors without compromising on their power densities and cycle life. This work explores the use of carbon soot as a potential porous and sustainable source of activated carbon materials as an electrode for supercapacitors. Thus, we explored carbon soot as a potential electrode material for supercapacitors using potassium bicarbonate as the activating agent and the activated carbon displayed a specific surface area of 61.85 m^2 g^{-1} and a capacitance of 83.2 F g^{-1} at a low current density of 0.5 Ag^{-1}. These results demonstrate the potential of this source of activated carbon for electrochemical applications.

5.2 Future Work

Although carbon soot is a suitable and a sustainable source of porous nanostructure electrode material for supercapacitor application as demonstrated using aqueous electrolytes in a three-electrode configuration, there is need to improve the voltage window between 2.4 -2.7 V for better capacitive performance. This can be achieved by using ionic or organic electrolytes on a full cell setup.

REFERENCES

Abedin, A., & Rosen, M. (2011). A Critical Review of Thermochemical Energy Storage Systems. *Open Renewable Energy Journal*, *4*, 42–46. https://doi.org/10.2174/1876387101004010042

Abruña, H. D., Henderson, J. C., & Kiya, Y. (2008). Batteries and Electrochemical Capacitors. *Phys. Today*, (12), 43–47. Retrieved from http://ecee.colorado.edu/~ecen4555/SourceMaterial/ElectricalEnerStor1208.pdf

Al, M., Gualous, H., Omar, N., & Van, J. (2012). Batteries and Supercapacitors for Electric Vehicles. In *New Generation of Electric Vehicles*. InTech. https://doi.org/10.5772/53490

Alexander, C., & Sadiku, M. (2007). *Fundamentals of Electric Circuits* (3rd ed.). McGraw-Hill. Bai, Y., Liu, M., Sun, J., & Gao, L. (2016). Fabrication of Ni-Co binary oxide/reduced grapheme oxide composite with high capacitance and cyclicity as efficient electrode for supercapacitors. *Ionics*, *22*(4), 535–544. https://doi.org/10.1007/s11581-015-1576-y

Ballantine, D. S., Martin, S. J., Ricco, A. J., Frye, G. C., Wohltjen, H., White, R. M., & Zellers, E. T. (1997). Materials Characterization. *Acoustic Wave Sensors*, 150–221. https://doi.org/10.1016/B978-012077460-9/50004-6

Béguin, F., Raymundo-Piñero, E., & Frackowiak, E. (2009). Electrical Double-Layer Capacitors and Pseudocapacitors (pp. 329–375). CRC Press. https://doi.org/10.1201/9781420055405-c8

Bokobza, L., Bruneel, J. L., & Couzi, M. (2014). Raman spectroscopy as a tool for the analysis of carbon-based materials (highly oriented pyrolitic graphite, multilayer graphene and multiwall carbon nanotubes) and of some of their elastomeric composites. *Vibrational Spectroscopy*, *74*, 57–63. https://doi.org/10.1016/j.vibspec.2014.07.009

Brezesinski, T., Wang, J., Tolbert, S. H., & Dunn, B. (2010). Ordered mesoporous alpha-MoO3 with iso-oriented nanocrystalline walls for thin-film pseudocapacitors. *Nature Materials*, *9*(2), 146–151. https://doi.org/10.1038/nmat2612

Brunauer, S., Emmett, P. H., & Teller, E. (1938). Adsorption of Gases in Multimolecular Layers. *Journal of the American Chemical Society*, *60*(2), 309–319. https://doi.org/10.1021/ja01269a023

Burke, A. (2000). Ultracapacitors: Why, How, and Where is the Technology. *Institute of Transportation Studies*. Retrieved from http://escholarship.org/uc/item/9n905017#page-7

Burke, A., & Zhao, H. (2015). Present and Future Applications of Supercapacitors in Electric and Hybrid Vehicles. *2015 IEEE 82nd Vehicular Technology Conference (VTC2015-Fall)*, (April), 1–5. https://doi.org/10.1109/VTCFall.2015.7391093

Castelvecchi, D. (2009). Spinning into control: High-tech reincarnations of an ancient way of storing energy. *Science News*, *171*(20), 312–313. https://doi.org/10.1002/scin.2007.5591712010

Chen, H., Cong, T. N., Yang, W., Tan, C., Li, Y., & Ding, Y. (2009). Progress in electrical energy storage system: A critical review. *Progress in Natural Science*, *19*(3), 291–312. https://doi.org/10.1016/j.pnsc.2008.07.014

Choi, M. Y., Hamins, A., Rushmeier, H., & Kashiwagi, T. (1994). Simultaneous optical measurement of soot volume fraction, temperature, and CO_2 in heptane pool fire. *Symposium (International) on Combustion*, *25*(1), 1471–1480. https://doi.org/10.1016/S0082-0784(06)80791-5

Confidential, C. (2012). Supercapacitors for Automotive & Other Vehicle Applications Automotive applications for Supercapacitors, (March), “The Kidwind Project : Using Mini-Supercapacitors.

Conway, B. E. (1999). *Electrochemical supercapacitors : scientific fundamentals and technological applications*. Berlin, Germany: Plenum Press. Retrieved from https://books.google.com/books?id=8yvzlr9TqI0C&pg=PA1

Dillon, E. C., Wilton, J. H., Barlow, J. C., & Watson, W. A. (1989). Large surface area activated charcoal and the inhibition of aspirin absorption. *Annals of Emergency Medicine*, *18*(5), 547–552. https://doi.org/10.1016/S0196-0644(89)80841-8

Dresselhaus, M. S., Jorio, A., Hofmann, M., Dresselhaus, G., & Saito, R. (2010). Perspectives on carbon nanotubes and graphene Raman spectroscopy. *Nano Letters*, *10*(3), 751–758. https://doi.org/10.1021/nl904286r

E. Frackowiak, F. B. (2001). Carbon Materials for the Electrochemical Storage of Energy in capacitors. *Journal of Carbon*, *39*, 937–950.

Elizabeth F. Rangel, S. M. da C. and, & Carvalho, B. M. (2017). World â€™ s largest Science , Technology & Medicine Open Access book publisher : *Design, Control and Applications of Mechatronic Systems in Engineering*, 135–152. https://doi.org/10.5772/67458

Ellenbogen, J. C. (2006). Supercapacitors : A Brief Overview, (March).

Fischer, U., Saliger, R., Bock, V., Petricevic, R., & Fricke, J. (1997). Carbon Aerogels as Electrode Material in Supercapacitors. *J. Porous Mater.*, *17*, 281. https://doi.org/10.1023/A:1009629423578

FREEMANTLE, M. (1998). DESIGNER SOLVENTS. *Chemical & Engineering News*, *76*(13), 32–37. https://doi.org/10.1021/cen-v076n013.p032

Frenklach, M., & Ebert, L. B. (1988). Comment on the proposed role of spheroidal carbon clusters in soot formation. *The Journal of Physical Chemistry*, *92*(2), 561–563. https://doi.org/10.1021/j100313a061

Gamby, J., Taberna, P. L., Simon, P., Fauvarque, J. F., & Chesneau, M. (2001). Studies and characterizations of various activated carbons used for carbon/carbon supercapacitors.

Journal of Power Sources, *101*(1), 109–116. https://doi.org/10.1016/S0378-7753(01)00707-8

Gardiner, D. J. (1989). Introduction to Raman Scattering. In *Practical Raman Spectroscopy* (pp. 1–12). Berlin, Heidelberg: Springer Berlin Heidelberg. https://doi.org/10.1007/978-3-642-74040-4_1

Gardner, J. (n.d.). Office of Energy Research, Policy and Campus Sustainability Overview of Compressed Air Energy Storage.

Garthwaite, J. (2011). How ultracapacitors work (and why they fall short). *Earth2Tech*. Retrieved from http://gigaom.com/cleantech/how-ultracapacitors-work-and-why-they-fall-short/

Hammarström, L., & Hammes-Schiffer, S. (2009). Artificial Photosynthesis and Solar Fuels. *Accounts of Chemical Research*, *42*(12), 1859–1860. https://doi.org/10.1021/ar900267k

Hanaor, D. A. H., Ghadiri, M., Chrzanowski, W., & Gan, Y. (2014). Scalable surface area characterization by electrokinetic analysis of complex anion adsorption. *Langmuir : The ACS Journal of Surfaces and Colloids*, *30*(50), 15143–52. https://doi.org/10.1021/la503581e

Haynes, B. S., & Wagner, H. G. (1981). Soot formation. *Progress in Energy and Combustion Science*, *7*(4), 229–273. https://doi.org/10.1016/0360-1285(81)90001-0

Hou, C.-H., Huang, J.-F., Lin, H.-R., & Wang, B.-Y. (2012). Preparation of activated carbon sheet electrode assisted electrosorption process. *Journal of the Taiwan Institute of Chemical Engineers*, *43*(3), 473–479. https://doi.org/10.1016/j.jtice.2011.12.003

Ke, Q., & Wang, J. (2016). Graphene-based materials for supercapacitor electrodes—A review. *Journal of Materiomics*, *2*(1), 37–54. https://doi.org/10.1016/j.jmat.2016.01.001

Kiamahalle, M. V., Cheng, C. I., Sata, S. A., Buniran, S., & Zein, S. H. S. (2011). Preparation and Capacitive Properties of Nickel-manganese Oxides/Multiwalled Carbon Nanotube/Poly (3,4-ethylenedioxythiophene) Composite Material for Electrochemical Supercapacitor.

Journal of Applied Sciences, *11*(13), 2346–2351.

https://doi.org/10.3923/jas.2011.2346.2351

Kim, J., & Ahn, S. (2015). Guest Editorial. *IEEE Transactions on Microwave Theory and*

Techniques, *63*(3), 778–779. https://doi.org/10.1109/TMTT.2015.2398752

Kötz, R., & Carlen, M. (2000). Principles and applications of electrochemical capacitors. *Electrochimica Acta*, *45*(15–16), 2483–2498. https://doi.org/10.1016/S0013-4686(00)00354-6

Kroics, K. (2015). System for start of an internal combustion engine with hybrid battery-supercapacitor source. In *2015 56th International Scientific Conference on Power and Electrical Engineering of Riga Technical University (RTUCON)* (pp. 1–6). IEEE. https://doi.org/10.1109/RTUCON.2015.7343167

Kumar, D., Agarwal, A. K., & Gupta, T. (2011). Effect of engine load on size and number distribution of particulate matter emitted from a direct injection compression ignition engine. *Aerosol and Air Quality Research*, *11*(7), 915–920. https://doi.org/10.4209/aaqr.2011.05.0070

Li, J., Yang, Q. M., & Zhitomirsky, I. (2010). Composite electrodes for electrochemical supercapacitors. *Nanoscale Research Letters*, *5*(3), 512–517. https://doi.org/10.1007/s11671-009-9518-0

Lin, F., Rothensteiner, M., Alxneit, I., van Bokhoven, J. A., & Wokaun, A. (2016). First demonstration of direct hydrocarbon fuel production from water and carbon dioxide by solar-driven thermochemical cycles using rhodium–ceria. *Energy Environ. Sci.*, *9*(7), 2400–2409. https://doi.org/10.1039/C6EE00862C

Liu, B. C., Li, F., Ma, L., & Cheng, H. (2010). Advanced Materials for Energy Storage, 28–62. https://doi.org/10.1002/adma.200903328

Luo, X., Wang, J., Dooner, M., & Clarke, J. (2015). Overview of current development in electrical energy storage technologies and the application potential in power system operation. *Applied Energy*, *137*, 511–536. https://doi.org/10.1016/j.apenergy.2014.09.081

Maryam, M., Suriani, A. B., Shamsudin, M. S., & Rusop Mahmood, M. (2012). BET Analysis on Carbon Nanotubes: Comparison between Single and Double Stage Thermal CVD Method. *Advanced Materials Research*, *626*, 289–293. https://doi.org/10.4028/www.scientific.net/AMR.626.289

Maxwell Technologies Ultracapacitors Regenerative Power. (n.d.). Maxwell.com. Retrieved from http://www.maxwell.com/products/ultracapacitors/applications/regenerative-power

McMullan, D. (2006). Scanning electron microscopy 1928-1965. *Scanning*, *17*(3), 175–185. https://doi.org/10.1002/sca.4950170309

Namisnyk, a M., Namisnyk, a M., Zhu, J. G., & Zhu, J. G. (n.d.). A SURVEY OF ELECTROCHEMICAL SUPERCAPACITOR TECHNOLOGY A.M. Namisnyk and J.G. Zhu Faculty of Engineering University of Technology, Sydney. *Engineering*, 1–6.

Omidvarborna, H., Kumar, A., & Kim, D. (2015). Recent studies on soot modeling for diesel combustion. *Renewable and Sustainable Energy Reviews*, *48*, 635–647. https://doi.org/10.1016/j.rser.2015.04.019

Rolda, S., Barreda, D., Granda, M., Mene, R., Santamarı, R., & Blanco, C. (2014). An approach to classification and capacitance expressions in electrochemical capacitors technology. https://doi.org/10.1039/C4CP05124F

Shabanzadeh, A. (2012). Production of activated carbon within the indirect gasification process.

Sharaf, O. Z., & Orhan, M. F. (2014). An overview of fuel cell technology: Fundamentals and applications. *Renewable and Sustainable Energy Reviews*, *32*, 810–853. https://doi.org/10.1016/j.rser.2014.01.012

Snook, G. A., Kao, P., & Best, A. S. (2011). Conducting-polymer-based supercapacitor devices and electrodes. *Journal of Power Sources*, *196*(1), 1–12. https://doi.org/10.1016/j.jpowsour.2010.06.084

Stanca, A. C., Borza, P. N., Romanca, M., Paun, R., & Zamfir, S. (2010). Model of supercapacitor-starter assembly used for internal combustion engines starting. In *2010 12th International Conference on Optimization of Electrical and Electronic Equipment* (pp. 943–948). IEEE. https://doi.org/10.1109/OPTIM.2010.5510526

Sung, T. ., Han, S. ., Han, Y. ., Lee, J. ., Jeong, N. ., Hwang, S. ., & Choi, S. . (2002). Designs and analyses of flywheel energy storage systems using high-Tc superconductor bearings. *Cryogenics*, *42*(6–7), 357–362. https://doi.org/10.1016/S0011-2275(02)00057-7

Supercapacitors for Military, Defence, Space, Isro, Spel,Capacitors, India'S First Supercapacitor, Ultracapacitors,. (n.d.). Retrieved September -29, 2017, from http://www.capacitorsite.com/defence.html

Tree, D. R., & Svensson, K. I. (2007). Soot processes in compression ignition engines. *Progress in Energy and Combustion Science*, *33*(3), 272–309. https://doi.org/10.1016/j.pecs.2006.03.002

Vuorilehto, K., & Nuutinen, M. (2014). Supercapacitors -basics and applications.

Wang, J., & Kaskel, S. (2012). KOH activation of carbon-based materials for energy storage. *Journal of Materials Chemistry*, *22*(45), 23710. https://doi.org/10.1039/c2jm34066f

Wang, L., Li, X., Guo, T., Yan, X., & Tay, B. K. (2014). Three-dimensional Ni(OH)2 nanoflakes/graphene/nickel foam electrode with high rate capability for supercapacitor applications. *International Journal of Hydrogen Energy*, *39*(15), 7876–7884. https://doi.org/10.1016/j.ijhydene.2014.03.067

Winter, M., & Brodd, R. J. (2004). What are batteries, fuel cells, and supercapacitors? *Chemical Reviews*, *104*(10), 4245–69. Retrieved from http://www.ncbi.nlm.nih.gov/pubmed/15669155

Wu, Z., Zhu, Y., Ji, X., & Banks, C. E. (2016). Transition Metal Oxides as Supercapacitor Materials (pp. 317–344). Springer, Cham. https://doi.org/10.1007/978-3-319-26082-2_9

Zhang, L. L., & Zhao, X. S. (2009). Carbon-based materials as supercapacitor electrodes. *Chemical Society Reviews*, *38*(9), 2520. https://doi.org/10.1039/b813846j

Zhong, C., Deng, Y., Hu, W., Qiao, J., Zhang, L., & Zhang, J. (2015). A review of electrolyte materials and compositions for electrochemical supercapacitors. *Chemical Society Reviews*, *44*(21), 7484–7539. https://doi.org/10.1039/c5cs00303b